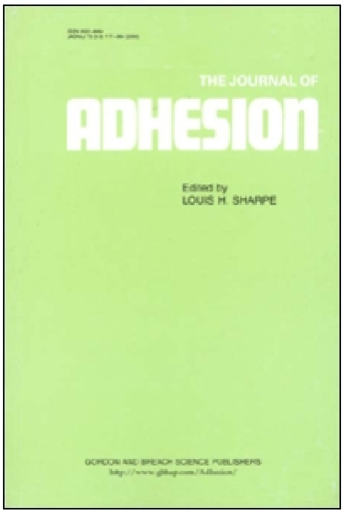

The Journal of Adhesion

Publication details, including instructions for authors and subscription information:
http://www.informaworld.com/smpp/title~content=t713453635

Adhesion Mechanisms of Polyurethanes to Glass Surfaces. III. Investigation of Possible Physico-Chemical Interactions at the Interphase

R. K. Agrawal[a]; L. T. Drzal[a]
[a] Department of Chemical Engineering, Composite Materials and Structures Center, Michigan State University, East Lansing, MI, USA

To cite this Article Agrawal, R. K. and Drzal, L. T.(1996) 'Adhesion Mechanisms of Polyurethanes to Glass Surfaces. III. Investigation of Possible Physico-Chemical Interactions at the Interphase', The Journal of Adhesion, 55: 3, 221 — 243
To link to this Article: DOI: 10.1080/00218469608009949
URL: http://dx.doi.org/10.1080/00218469608009949

J. Adhesion, 1996, Vol. 55, pp. 221–243
Reprints available directly from the publisher
Photocopying permitted by license only

Amsterdam B.V. Published in The Netherlands
under license by Gordon and Breach Science
Publishers SA
Printed in Malaysia

Adhesion Mechanisms of Polyurethanes to Glass Surfaces. III. Investigation of Possible Physico-Chemical Interactions at the Interphase

R. K. AGRAWAL and L. T. DRZAL*

Department of Chemical Engineering, Composite Materials and Structures Center, Michigan State University, East Lansing, MI 48824, USA

(Received December 16, 1994; in final form June 7, 1995)

Surface free energies of polyurethanes made from toluene diisocyanate and 1,4 butanediol-based hard segments and caprolactone polyol-based soft segments were calculated using additive functions. Good agreement was found between the calculated values based on additive functions and the calculated values based on contact angle measurements. The phase-separated polyurethanes were found to have a higher polar surface free energy component (γ^P). This was linked to the preferential segregation of butanediol/butanediol-derived moieties to the polyurethane surfaces due to phase separation. The adhesion values of these polyurethanes to soda-lime glass were correlated with their respective γ^P values and a linear relationship was found. It was also shown that the adhesion values of the low γ^P polyurethanes improved substantially when the glass surfaces were coated with a thin layer of butanediol prior to the bonding. The modulus of the interphase region rich in butanediol was evaluated. Although a modulus increase was found at the interface, this increase was found to play a secondary role in the adhesion. The chemical interactions at the polyurethane/glass interphase were investigated by pre-treating the glass surfaces with methyltrimethoxysilane and trimethylchlorosilane prior to adhesion testing. The adhesion data showed no significant difference between the uncoated and the silane-treated glass substrates. Based on this experimental evidence, the possibility of any covalent or ionic bonding at the polyurethane/glass interphase was assumed negligible. It was determined that the mechanism of adhesion between the polyurethanes and the glass surface could be through the formation of an interphase region in which hydrogen bonding between the butanediol-rich interphase region and the hydroxylated glass surface plays a key role.

KEY WORDS: Polyurethanes; adhesion; glass; interphase; surface free energy; chemical and physical interactions.

INTRODUCTION

Glass/polyurethane adhesion has become increasingly important in the automotive and other industries in a variety of applications including laminated windshields, reaction injection molded modular windows for automobiles, long and short glass fiber reinforced thermoplastic and thermoset composites, etc. Also, the use of polyurethane coatings on the inside glass surface of windshields is being investigated to impart an

---

* Corresponding author.

antilacerative property to the windshield to protect occupants in the event of a collision. In all of these applications, good adhesion between the glass and the polyurethane is imperative.

Adhesion between two dissimilar surfaces such as glass and polyurethane is regarded as a complex phenomenon influenced by many factors including physical and chemical interactions. The reversible physical interactions are caused by van der Waals forces which may also include hydrogen bonding. The irreversible chemical interactions may include ionic and covalent bond formation across the interface between the two materials.

Several researchers have studied polyurethane surfaces to determine the surface compositions and surface properties. Vargo *et al.*[1] have found that the polyurethane surface is enriched in the low molecular weight polyether component. Sengupta *et al.*[2] have determined the polar and the dispersive components of the surface free energies of polyurethanes and have tried to relate these to the surface soft segment contents.

The glass surface is also very complex reflecting its composition and history of environmental exposure. Fowkes *et al.*[3] have used the acid-base interaction approach to study adhesion of glass to various polymers. The chemical composition of the surface of glass has also been studied by several authors using x-ray photoelectron spectroscopy and other surface-sensitive techniques.[4–8] The research indicates that glass surfaces, exposed to ambient atmosphere, are enriched in sodium ions relative to the bulk. Glass surfaces are usually found to be hydrated due to the adsorption of water vapor. It has also been suggested that $NaHCO_3$-type species may be present on the surface due to the adsorption of carbon monoxide and dioxide species from the atmosphere.

All of the studies mentioned above have addressed either the surface composition of the polyurethanes or the glass surfaces but have done little to correlate the actual chemical and physical nature of the interface with adhesion of these polyurethanes to the glass surfaces.

In our previous studies on glass/polyurethane adhesion[9–10] we found that polyurethane-to-glass adhesion is greatly influenced by the modulus of the polymer in the interphase. We also found that, along with modulus, phase separation in polyurethane influences its adhesion to glass. An interphase region was found between the polyurethane matrix and the glass substrate of our previous studies which had a composition intermediate to that of the matrix and the glass surface. The composition and the thickness of this interphase region was found to be related to the phase separation in the matrix.

In the present study, we have investigated the physico-chemical interactions at the polyurethane/glass interface. Surface free energies of the various polyurethane formulations were evaluated using theoretical and experimental techniques, and the dependence of the surface free energies on the surface composition and/or the phase separation has also been studied. The work of adhesion to the glass surface has been evaluated for the various phase-mixed and phase-separated polyurethanes and compared with the experimental adhesion data reported earlier.[9] The role of chemical interactions at the polyurethane/glass interface has been explored by coating the glass surfaces with an alkyl silane to make the surface chemically "inert" prior to the adhesion testing.

EXPERIMENTAL

Materials

The polyurethanes used in this study were based on caprolactone polyols available from Union Carbide under the trade name "Tone". Hard segments were made from a 80–20% mixture of toluene 2,4-diisocyanate and toluene 2,6-diisocyanate (TDI, Aldrich Chemical Co.) and 1,4-butanediol (BDO, Aldrich Chemical Co.) as the chain extender. The various polyurethane formulations studied in this work and the previous work are shown in Table I.

For adhesion testing, annealed soda-lime float glass plaques were used. A typical soda-lime float glass plaque has two sides, an air side and a tin side. The air sides of the glass plaques were used for the adhesion testing. 1/4″ × 1/4″ × 1/4″ (6.4 × 6.4 × 6.4 mm) blocks of polyurethanes were cast on the air side of the glass plaques. The details of polyurethane mixing and adhesion sample preparation can be found in our previous study.[9]

Surface Energy Measurements

The various polyurethane formulations were cast on clean 75 × 50 mm glass slides. The samples were then heated for 24 hours at 90°C in a convection oven. The final polyurethane coating thickness on the glass slides was about 1 to 2 mm. The glass slides were handled carefully throughout the sample preparation to avoid any surface contamination of the polyurethane surfaces.

The surface free energies of the samples thus prepared were calculated using the experimentally-determined contact angles of sessile drops using a Ramé-Hart Model 100 goniometer. All experiments were conducted at room temperature ($\sim 23°C$). The data were obtained for wetting by a series of fluids with varying surface tensions which are shown in Table II.[11] The liquids used covered a wide range of polarities from low, such as α-bromo-naphthalene, to high, such as water. This allowed us to develop a

TABLE I
Urethane formulations at isocyanate index of 1.0

Sample designation	Polyol			BDO (Mol%)	TDI (Mol%)	Hard segment	Molecular weight per cross-link (M_c)
	Tone 0301	Tone 0305	Tone 0310				
10A	–	–	X	0	60	22	1160
10B	–	–	X	22	56	37	1424
10C	–	–	X	31	54	47	1692
10D	–	–	X	34	53	60	2222
10E	–	–	X	41	52	67	2752
5B	–	X	–	7	58	37	854
5C	–	X	–	20	56	47	1013
5D	–	X	–	31	54	59	1324
5E	–	X	–	36	53	67	1646
1C	X	–	–	0	60	47	563
1D	X	–	–	18	57	59	739
1E	X	–	–	26	55	67	912
HS	–	–	–	50	50	100	–

TABLE II
Surface free energies of liquids used for contact angle measurements[11]

Liquid	Surface free energy (dynes/cm)		
	γ^D	γ^P	γ
Water	21.8	51.0	72.8
Glycerol	37.0	26.4	63.4
Formamide	39.5	18.7	58.2
Methylene iodide	48.5	2.3	50.8
α-bromonapthalene	44.6	0.0	44.6

comprehensive wettability profile for each polyurethane formulation. Liquids with very low surface tensions, such as *n*-alkanes, were not used in this study due to the difficulty and errors associated with measuring small ($<10°$) contact angles.

Dynamic Mechanical Analysis

Rectangular bars (30 mm × 4 mm × 1.5 mm) of polyurethane samples were used for dynamic mechanical analysis on a Polymer Laboratories MK III DMTA system. Elastic storage moduli (E') at various temperatures were obtained in a single cantilever bending oscillation mode of deformation at 1 Hz fixed frequency. The temperature was varied from 10°C to 50°C at 5°C/min.

Glass Pretreatment

A 2.0 weight percent solution of methyltrimethoxysilane, available from Dow Corning under the trade name Z 6070, was prepared in reagent grade methanol. Approximately 10 weight percent (of the amount of Z 6070) deionized water was added to the solution and the solution was aged for a week prior to use. Another 2.0 weight percent solution of trimethylchlorosilane, available from Aldrich Chemical Co., was prepared in reagent grade tetrahydrofuran. Cotton swabs were used to apply an even coating of these solutions to the air side of the soda-lime glass plaques. The coated glass plaques were allowed to dry for 30 minutes and then were used to prepare polyurethane adhesion samples.

X-Ray Photoelectron Spectroscopy (XPS)

Subsequent to adhesion testing, failed glass surfaces were analyzed using a Perkin-Elmer PHI 5400 x-ray photoelectron spectrometer. An approximately 6.4 × 6.4 mm square area was sectioned from the failed glass surface and was placed inside the XPS chamber. The angle-dependent XPS spectra were obtained at a base pressure of approximately 10^{-9} Torr. The standard Mg K_α source was used for all sample analysis and was operated at 300 W (15 kV, 20 mA). A continuously-variable-angle sample stage was used and was programmed for 15°, 45°, and 90° angles (photoelectron take-off angle). The surface area of the sample analyzed by the spectrometer is set through an initial lens system and was set for a 2.0 mm diameter circle. Data were collected in the fixed analyzer transmission mode using a position-sensitive detector and a 180°

hemispherical analyzer. Pass energies were set at 89.45 eV for the survey scans (0–1000 eV) and at 35.75 eV for the narrow scans of the elemental regions. Data collection and manipulation were performed with an Apollo 3500 workstation running PHI ESCA software. The curve fitting was carried out using a modified Gauss-Newton nonlinear least squares optimization procedure that is part of the instrumental software. The C 1s binding energy of the graphitic peak was set to 285.0 eV for calibration purposes.

ESTIMATION OF POLYURETHANE SURFACE FREE ENERGY

The surface free energy of the polyurethanes of this study can be estimated using an approach described by Eberhardt.[12] According to Eberhardt, the surface free energy of polyurethanes can be expressed as:

$$\gamma_U = N_S\gamma_S + N_H\gamma_H$$

where γ_U is the total surface free energy of the polyurethanes, N_S and N_H are the mole fractions of the soft and the hard segments on the surface of the polyurethanes and the γ_S and γ_H are the surface free energies of the soft and the hard segments, respectively. The γ_S can be estimated using an empirical relationship.[11]

$$\gamma_S \approx 0.75\,(e_{\text{coh}})^{2/3}$$

where γ_S is expressed in dynes/cm and the cohesive energy density, e_{coh}, in J/cm^3. A material's solubility parameter is defined as the square root of its cohesive energy density. The solubility parameter of caprolactone based polyols is $\delta_s = 18.6$ (J/cm^3)$^{1/2}$.[13] Thus,

$$\gamma_S \approx 0.75\,(\delta_S^2)^{2/3}$$

$$\gamma_S \approx 37.0\,\text{dynes/cm}$$

The γ_H can be estimated by an additive function, the molar parachor, P_S, as proposed by Sugden[14] and discussed by Van Krevelen.[11] The γ_H was calculated to be 49.2 dynes/cm. The details of this calculation are shown in Appendix A.

Assuming that the surface composition is the same as the bulk composition, the N_S and the N_H values can be calculated from the various polyurethane's stoichiometric formulations and are listed in Table III. Based on the N_S, N_H, γ_H, and γ_S values, the γ_U for the various polyurethanes were calculated and are shown in Table III. It should be noted that as the hard segment content increases in the polyurethanes, the γ_U values also increase being the highest for the 100% hard segment content sample HS.

RESULTS AND DISCUSSION

Physical Interactions

The surface free energies of the various model polyurethanes were determined from the contact angle measurements of several liquids with different surface tensions and chemical functionalities. Zisman[15] plots of cos θ *versus* γ were developed for all the polyurethane samples. Figures 1a and 1b show the sample Zisman plots for polyurethane sample 1C with 46.7 wt.% hard segment and sample HS with 100 wt. % hard segment. The extrapolated critical surface tension, γ_C, at cos $\theta = 1$ for all the samples are shown in Table IV. The γ_C signifies the empirical value of the maximum surface tension of liquids able to spread on the given surface. The γ_C data reveal that the critical surface tension of the various polyurethanes studied are close to each other, considering the experimental errors involved in the measurements. Also, no clear trend in the data with

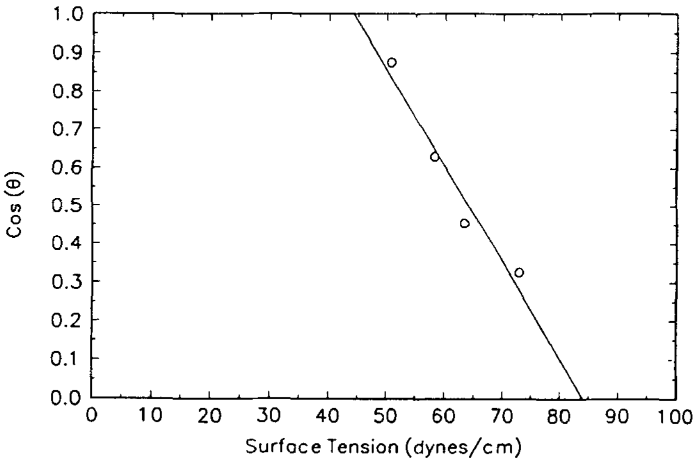

(a)

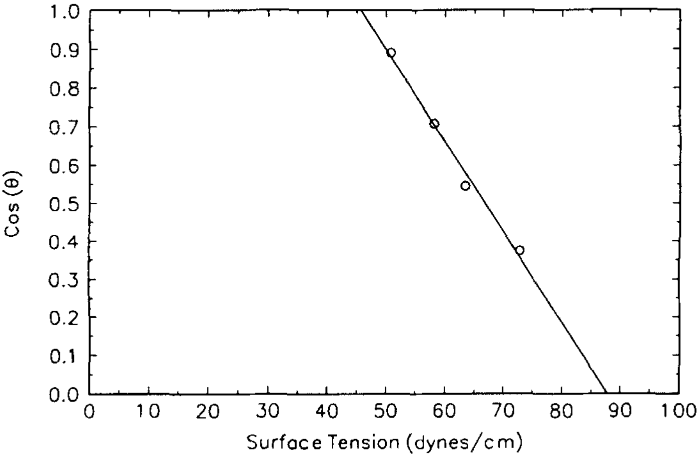

(b)

FIGURE 1 Zisman plots of (a) 1C polyurethane sample with 46.7 wt. % hard segment and (b) HS polyurethane sample with 100% hard segment.

TABLE III
Calculated surface free energies of the polyurethanes based on molar parachors

Samples	Mole fraction		Surface free energy (dynes/cm)
	N_S Soft segment	N_H Hard segment	γ_U
10A	0.401	0.599	44.3
10B	0.222	0.778	46.5
10C	0.154	0.846	47.3
10D	0.132	0.868	47.6
10E	0.069	0.931	48.4
1C	0.398	0.602	44.3
1D	0.260	0.740	46.0
1E	0.194	0.806	46.8
HS	0.0	1.0	49.2

increasing hard segment content can be observed, as was inferred from the surface free energies calculated from molar parachors.

Along with the critical surface free energy, polar and dispersive components of the surface free energies of these polyurethanes were also evaluated from the contact angle measurements. According to Schultz *et al.*,[16] the surface free energy can be represented by the sum of two components, namely a dispersion (γ^D) and a polar component (γ^P).

$$\gamma = \gamma^D + \gamma^P$$

The $(\gamma_L^P/\gamma_L^D)^{1/2}$ and $\gamma_L(1+\cos\theta)/2(\gamma_L^D)^{1/2}$ values for the various polyurethanes were plotted and $(\gamma_U^P)^{1/2}$ and $(\gamma_U^D)^{1/2}$ values were obtained from the slope and the intercept of the linear regression fit lines through the experimental data points.[17-19] One such plot for Tone 0310-based polyurethanes is shown in Figure 2. From the graph, we see that as the hard segment content increases in these samples, their slopes also increase. This indicates that as the hard segment content increases, the polar component of the polyurethane surface free energy also increases. The γ^P and γ^D values obtained from these graphs are shown in Table IV. The last column in Table IV also shows the overall surface free energy of these polyurethanes (γ_U) which is the sum of the γ^P and γ^D values.

Figure 3 shows the graphs of calculated γ_U values based on molar parachors and contact angle measurements *versus* the hard segment content in the Tone 0310-based polyurethanes. Both the graphs show the same trend that the surface free energy increases with the increasing hard segment content. The molar-parachor-based values are in good agreement with the contact-angle-measurement-based values. They are higher than the contact-angle-measurement-based values by only 3–4 dynes/cm and the difference is less for the higher hard segment content samples (10D, 10E, etc.) which are phase-separated polyurethane systems.[9-10] This small amount of difference could be due to the assumption made in the molar-parachor-based calculations regarding the surface composition being the same as the bulk composition. The contact-angle-measurement-based γ_U curve shows an increase in the value after the sample 10C and then maintains the high γ_U values for the samples 10D, 10E, and HS. This sharp rise in γ_U values could be due to the phase separation in these samples leading to the surface

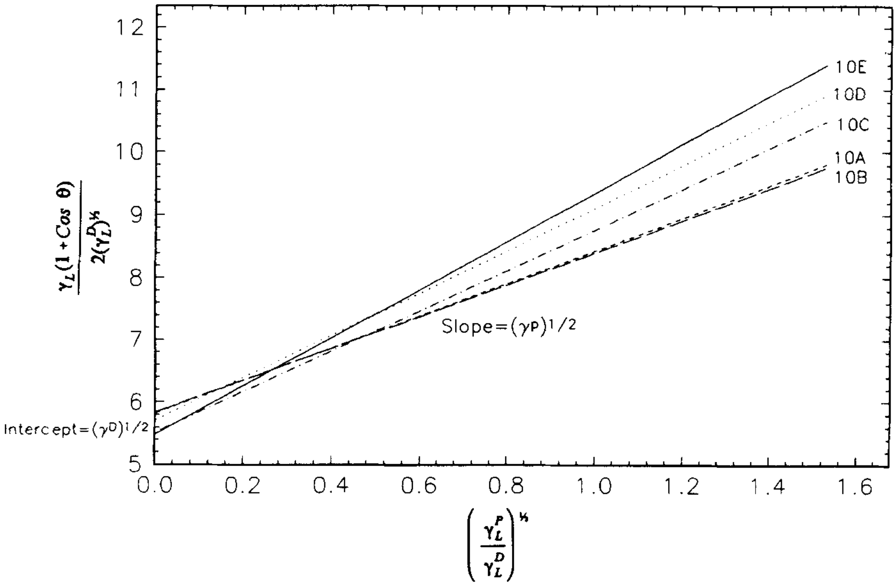

FIGURE 2 $\left(\frac{\gamma_L^P}{\gamma_L^D}\right)^{1/2}$ vs. $\frac{\gamma_L(1+\cos\theta)}{2(\gamma_L^D)^{1/2}}$ plot for Tone 0310 based polyurethanes with different hard segment contents.

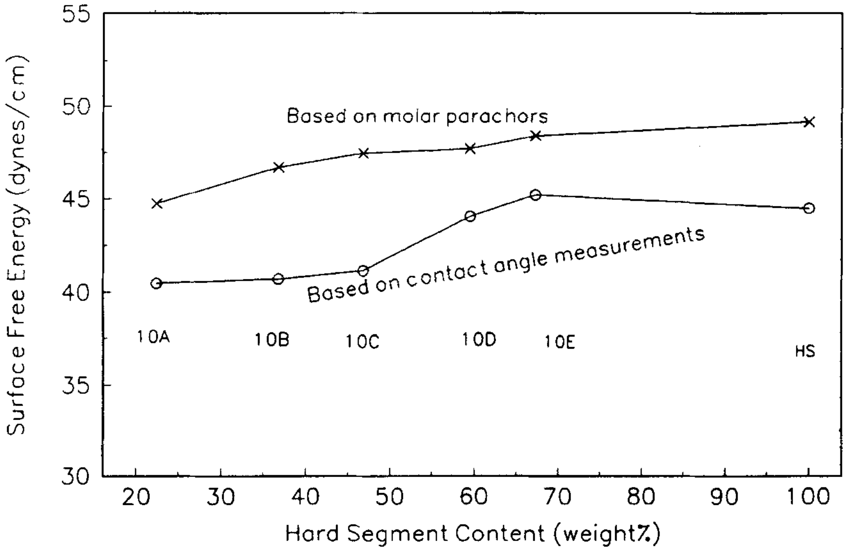

FIGURE 3 Surface free energy values of Tone 0310 based polyurethanes with different hard segment contents.

enrichment in high surface free energy species. This is further explored by plotting the polar component of the surface free energy for these samples.

Figure 4 shows the γ^P *versus* hard segment content for Tone 0310 and Tone 0310 based polyurethanes. Also shown is the data point HS for the 100% hard segment content polyurethane (contains only BDO and TDI). The data show that the γ^P values increase with increasing hard segment content in both the 1 and 10 series polyurethane samples. The γ^P values for the 1 series are in general lower than those for the 10 series for the same hard segment contents. A sharp increase in the γ^P value of sample 10C is also observed and the trend continues with samples 10D and 10E. This observation can be explained by noting that with increasing hard segment content, phase separation increases in higher molecular weight polyol (Tone 0310) based polyurethanes.[9-10] The phase separation in the lower molecular weight polyol (Tone 0301) based polyurethanes is not as significant and thus the γ^P values for these polyurethanes are lower than for the 10 series polyurethanes. The γ^P value for the 100% hard segment content polyurethane is 8.7 dynes/cm which is lower than the γ^P values for the samples 10C, 10E, and 10E, all of which have lower hard segment content. The higher γ^P values for 10C, 10D, and 10E suggests that the surfaces of these polyurethanes are not rich in the hard segment. Further, the higher γ^P values can be explained by the phase separation in these polyurethanes. In our previous studies,[9-10] we have discussed phase separation in these polyurethanes and have shown that, due to phase separation, the surface composition in these polyurethanes tends to be rich in hydroxyl-containing species and

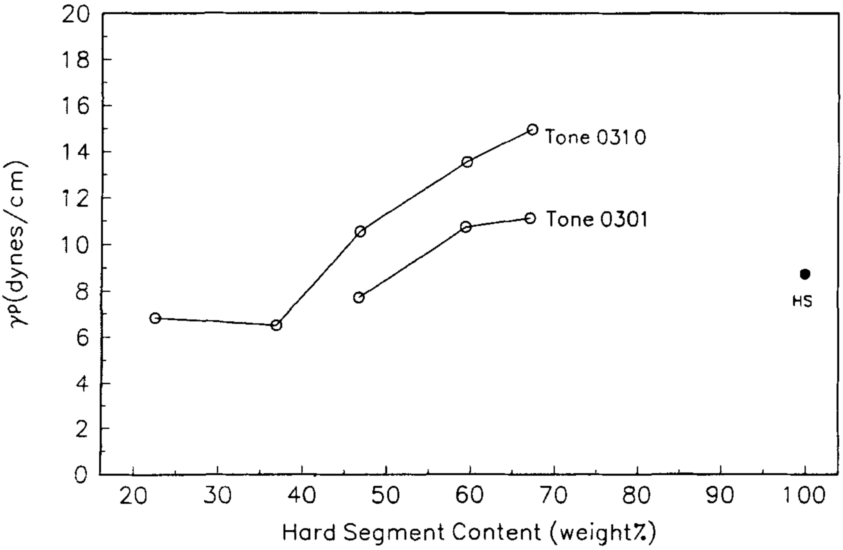

FIGURE 4 Polar component of surface free energy for various polyurethanes with different hard segment contents.

TABLE IV
Calculated surface free energies of the polyurethanes based on contact angle measurements

Samples	Surface free energy (dynes/cm)			
	γ_C	γ^P	γ^D	$\gamma_V = (\gamma^P + \gamma^D)$
10A	44.4	6.8	33.6	40.4
10B	44.0	6.5	34.2	40.7
10C	44.6	10.6	30.6	41.2
10D	44.3	13.6	30.5	44.1
10E	42.2	15.0	30.3	45.3
1C	41.83	7.7	34.2	41.9
1D	42.46	10.7	32.5	43.2
1E	42.76	11.1	32.5	43.6
HS	43.64	8.7	35.8	44.5
Glass	–	37.6	19.2	56.8

deficient in nitrogen-containing groups when compared with the stoichiometric composition. The two hydroxyl-containing species in these polyurethanes are the polyols and the chain extender (BDO). Due to the lower molecular weight of the chain extender, it is more likely to come to the surface.[10] This is also supported by the γ^P values observed here. The lower γ^P value samples 10A, 1C, and 10B have no, or very small, BDO content and also poor phase separation and, thus, their surfaces are not rich in BDO. On the other hand, in the samples 10D and 10E, BDO segregates to the surface and results in higher γ^P values. The surface free energy values for BDO are:[13]

$$\gamma^P = 14.6\,\text{dynes/cm}$$

$$\gamma^D = 29.6\,\text{dynes/cm}$$

$$\gamma = 44.2\,\text{dynes/cm}$$

The γ^P of the polyols is expected to be less than 14.6 due to higher hydrocarbon content and this further supports the conclusion that the surfaces of these polyurethanes are rich in BDO.

The adhesion values of these polyurethanes to soda-lime glass surface were determined previously[9] and are shown in Table V. We had shown that the polyurethane-to-glass adhesion improved with phase separation in the matrix and also with the modulus of the matrix. A plot of the adhesion values as a function of γ^P is shown in Figure 5. A linear relationship can be seen between the γ^P and the adhesion values.

The above observations suggest that in the samples exhibiting good adhesion to the glass, the interphase region between the polyurethane matrix and the glass surface [10] consists of a larger concentration of higher polar free energy components than the bulk and the components are butanediol-type species. These chemical species can experience hydrogen bonding with the hydroxyl-rich glass surface.

To explore further the role of the hydrogen bonding and other polar interactions between the polyurethane surface and the glass surface, an additional adhesion experiment was conducted. In this experiment, selected polyurethanes with varying surface γ^P values (and thus with varying surface BDO content) were bonded to the bare soda-lime glass plaques and to glass plaques coated with 2% (weight) layer of BDO

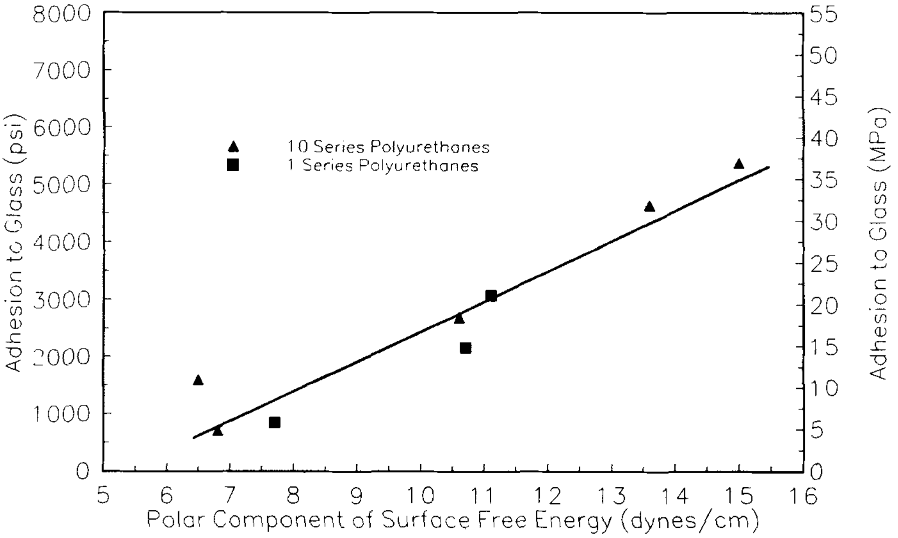

FIGURE 5 Adhesion to Glass versus polar component of the surface free energy for various polyurethane systems.

from acetone. The samples were tested for adhesion values in a shear mode (details of adhesion testing are discussed in Ref. 9) and the data are shown in Table VI. The data reveal that the adhesion values of the polyurethanes with low γ^P values can be significantly improved by coating the glass surface with BDO or, in other words, by making their surface rich in the higher γ^P component, BDO.

TABLE V
Work of adhesion between the polyurethanes and the glass surface

Samples	W_{adh} (dynes/cm)	Shear adhesion (psi)[9]/(Mpa)
10A	83	706 ± 4 (4.9 ± 0.03)
10B	83	1590 ± 30 (11.3 ± 0.2)
10C	88	2690 ± 60 (18.8 ± 0.4)
10D	92	4640 ± 80 (32.5 ± 0.6)
10E	96	5370 ± 300 (37.6 ± 2.1)
1C	85	825 ± 340 (5.8 ± 2.4)
1D	90	2120 ± 530 (14.8 ± 3.7)
1E	91	3020 ± 1360 (21.1 ± 9.5)
HS	89	–

The failed glass surfaces after the adhesion testing were analyzed using XPS. Figure 6 shows the curve-fitted C 1s spectra of sample 1D and sample 1D with the glass surface coated with BDO, taken at 15° photoelectron take-off angle. These spectra have been charge corrected with the C—C peak referenced to 285.0 eV. A cursory look at the spectra reveals that there are several binding states of carbon present on the samples, both at higher and at lower binding energies of C—C bonds (285.0 eV). The C 1s peak binding energies and the relative peak areas are shown in Table VII. The peak at ~289.5 eV can be associated with the polyurethane linkage[10] and its presence indicates a cohesive mode of failure in both the samples. The higher polyurethane peak area in the BDO-coated glass surface indicates a surface richer in polyurethane than the 1D glass surface without the BDO coating. The peak ~286.5 eV can be due to the un-reacted free hydroxyls, C—OH, from the polyol and BDO. The significantly higher area fraction for this peak in the BDO-coated adhesion sample, as compared with the uncoated adhesion sample, suggests the presence of partially or completely unreacted BDO on the surface. Thus, we can conclude that some BDO molecules from the coating react with isocyanates to form polyurethane linkages and become part of the matrix while others remain unreacted.

It is conceivable that the unreacted BDO molecules present in the interphase region of BDO-coated glass adhesion samples can lead to localized change in the mechanical properties of the interphase region. The modulus of the modified interphase region could influence the adhesion of the matrix in addition to the hydrogen bonding mentioned earlier. To understand the mechanical properties of the butanediol-rich interphase region, polyurethane rectangular bars were prepared with 5% and 15% (by total weight) excess of 1,4 butanediol. The excess BDO was incorporated into the urethane composition. Excess BDO was blended into the polyol prior to the isocyanate addition. In the second method, excess BDO was added to a homogeneous stoichiometric mixture of polyol, BDO, and isocyanate. It is expected that the urethane produced would closely represent the interphase formation process in the experimental samples used in this study. The samples with 15% excess butanediol did not cure well, and the samples were either tacky and "putty-like" or very brittle with poor tensile properties. These samples could not be tested for mechanical properties. The samples with 5% excess butanediol were tested for elastic storage modulus using Dynamic Mechanical Analysis and the data are shown in Table VIII. Also shown in Table VIII is the elastic storage modulus for the corresponding polyurethane with the stoichiometric formulation.

The data indicate that the elastic storage modulus of polyurethane 1D with 5% excess BDO is about 10%–12% higher than for the stoichiometric composition 1D. Since the interphase formation in BDO-coated glass plaques is expected to be simulated by this method, we can conclude that the localized interphase modulus in the BDO-coated 1D adhesion sample is higher than that in the uncoated 1D adhesion sample. Based on the observations from our previous study[9] which concluded that a higher interphase modulus results in higher adhesion values, these adhesion results obtained with BDO-coated glass plaques are in agreement. This observation suggests that the preferential segregation of BDO type species to the interphase region in polyurethane/glass samples influences its adhesion not only through increased polar interactions and hydrogen bonding but also by increasing the modulus of the interphase region.

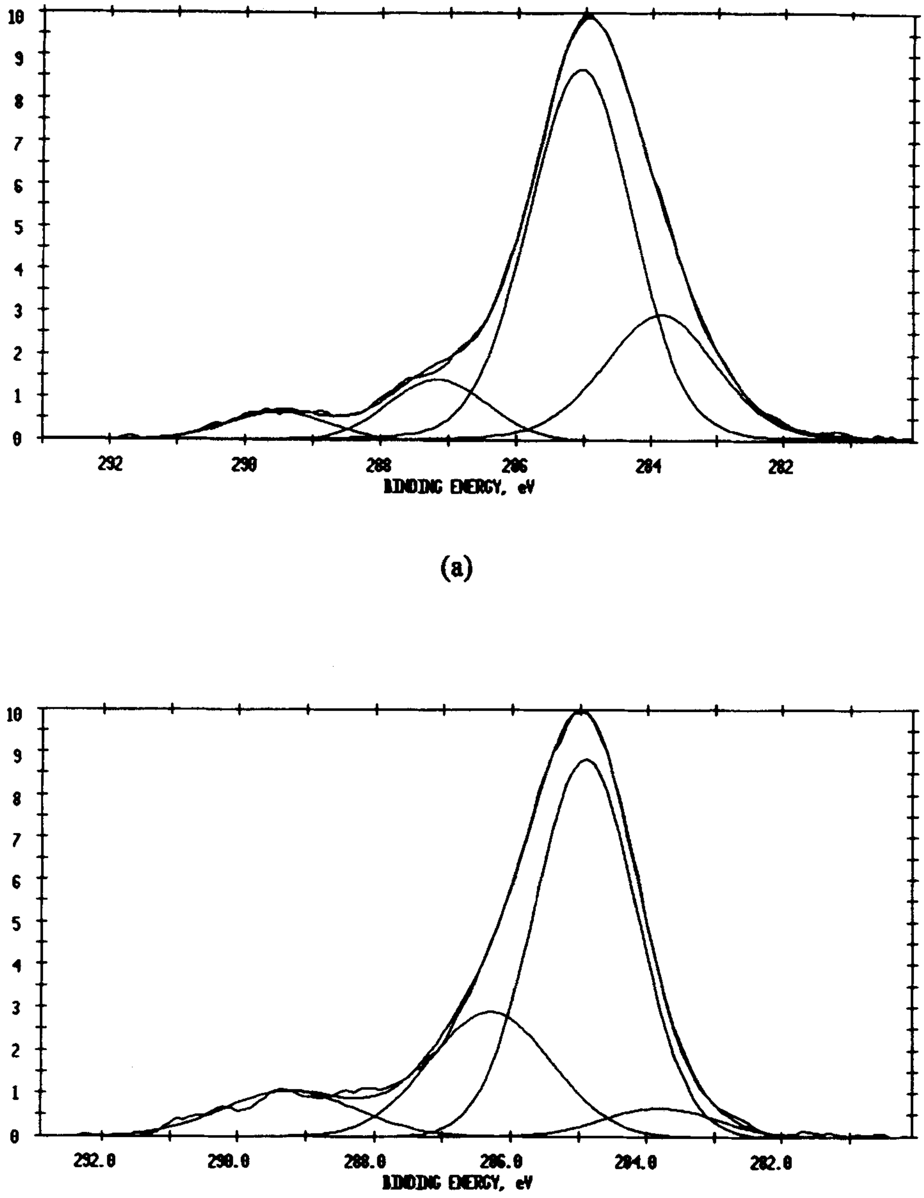

FIGURE 6 Curve fitted C 1s spectra of failed glass surfaces taken at 15° photoelectron take-off angle (a) Sample 1D (b) Sample 1D with BDO-coated glass.

TABLE VI
Adhesion values of various polyurethanes to bare glass surface and to 1,4 butanediol coated glass surface

Samples	2% Secant shear[9] modulus iosipescu Testing (psi)/(GPa)	γ^P (dynes/cm)	Relative BDO concentration on the surface (Arbitrary units)	Adhesion to bare glass surface (psi)/(MPa)	Adhesion to 1,4 butanediol coated glass surface (psi)/(MPa)
10D	151×10^3 (1.06)	13.6	+ + +	4640 ± 80 (32.5 ± 0.6)	4550 ± 80 (31.8 ± 0.6)
1D	185×10^3 (1.29)	10.7	+ +	2120 ± 530 (14.8 ± 3.7)	4980 ± 850 (34.9 ± 5.9)
1C	176×10^3 (1.23)	7.7	+	825 ± 340 (5.8 ± 2.4)	4120 ± 130 (28.8 ± 0.9)
10B	1400* (0.010)	6.5		1590 ± 30 (11.1 ± 0.2)	1510 ± 50 (10.6 ± 0.4)

* Tensile Modulus, sample was too soft for Iosipescu testing

TABLE VII
C 1s peak binding energies and relative peak areas of carbon chemical states on failed glass samples

Sample	Peak I		Peak II		Peak III		Peak IV	
	B.E. (eV)	Area (%)	B.E. (eV)	Area (%)	B.E. (eV)	Area (%)	B.E. (eV)	Area (%)
1D	283.76	23.90	285.13	62.81	286.98	9.11	289.46	4.17
1D with BDO coating on Glass	283.80	5.07	284.91	61.57	286.3	23.87	289.24	9.48

TABLE VIII
Elastic storage modulus of various polyurethanes at different temperatures

Temperature (°C)	Elastic storage modulus (psi)/(GPa)	
	1D	1D with 5% excess BDO
10	390×10^3 (2.73)	438×10^3 (3.07)
15	381×10^3 (2.67)	438×10^3 (3.07)
20	381×10^3 (2.67)	428×10^3 (2.94)
25	381×10^3 (2.67)	418×10^3 (2.87)
30	373×10^3 (2.61)	418×10^3 (2.87)
35	364×10^3 (2.55)	399×10^3 (2.80)
40	356×10^3 (2.49)	390×10^3 (2.73)
45	348×10^3 (2.44)	373×10^3 (2.61)
50	348×10^3 (2.44)	356×10^3 (2.49)

The work of adhesion due to the polar and the dispersive interactions was also calculated for the various polyurethanes/glass systems using Kaelble's expression.[20] Kaelble has modified the expression originally developed by Good[21] and Fowkes[17] and has represented it as the sum of the work due to the dispersion and the polar components.

$$W_{\mathrm{adh}} = W^{D}_{\mathrm{adh}} + W^{P}_{\mathrm{adh}}$$

Using the geometric mean relation to predict the interactions,

$$W_{\mathrm{adh}} = 2\,[(\gamma^{D}_{U}\gamma^{D}_{G})^{1/2} + (\gamma^{P}_{U}\gamma^{P}_{G})^{1/2}]$$

We obtained the W_{adh} values for the polyurethane/glass systems and they are shown in Table V. A quantitative comparison between the calculated work of adhesion and the measured adhesion values in terms of the load required to induce bond failure is not relevant, but a qualitative comparison of the trends in the data can provide valuable information. The data show that W_{adh} increases slightly with increasing hard segment content but not to the extent observed in the experimental adhesion data. The shear adhesion data increase from 706 psi (4.87 MPa) for sample 10A, with 22 weight percent hard segment content to 5370 psi (37.0 MPa) for sample 10D, with 67 weight percent hard segment content. The lack of agreement between the calculated W_{adh} and the experimental adhesion data may be explained by the recent observations made by Fowkes *et al.*[3] that the geometric mean relation may not include the effects of hydrogen bonding at the interface which might be an important factor in the polyurethane/glass systems. Another reason for this discrepancy can be the fact that the W_{adh} calculation does not take into consideration the effects of matrix modulus on adhesion.

Chemical Interactions

Glass surfaces are known to be rich in isolated, vicinal and geminal silanol groups. In addition to the physical interactions between the surface silanols and the polyurethane matrix, there could be various chemical interactions. To investigate the chemical interactions such as covalent and ionic bonding, the glass surfaces were pre-treated with two different silane coupling agents. A 2% (by weight) solution of prehydrolyzed methyltrimethoxylsilane and a 2% (by weight) solution of trimethylchlorosilane in tetrahydrofuran were used to pretreat glass surfaces prior to the adhesion testing. The purpose of the silane treatment was to make the otherwise hydroxylated glass surface chemically inert towards any subsequent covalent bond formation with polyurethanes. Another function of the silane coating was to provide a barrier layer between the glass and the polyurethane matrix to avoid any possibility of ionic bond formation between the Na^{+}, K^{+}, and Ca^{++} ions and the polyurethane matrix. On the other hand, the silane coatings could also influence wettability of the various polyurethanes by providing potentially lower energy surfaces. However, Plueddemann[22] had shown than little correlation existed between the surface free energy of silanes and their effectiveness as coupling agents between glass and polymeric matrices. The polyurethanes of this study showed adequate wetting to the silane treated glass surfaces. Shown in Figure 7a and 7b are the idealized monolayers of the condensed methyltrimethoxysilane and trimethylchlorosilane on glass surfaces, respectively.

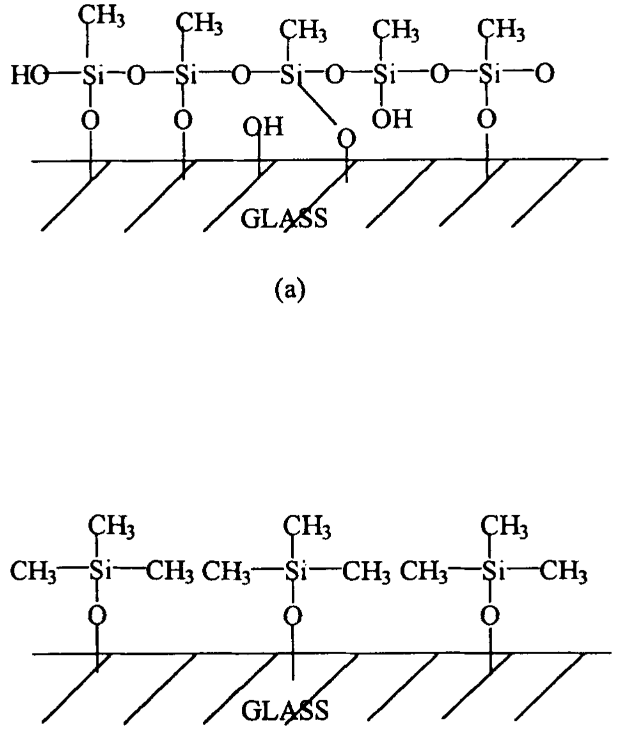

(a)

(b)

FIGURE 7 Idealized monolayer of condensed (a) methyltrimethoxysilane and (b) trimethylchlorosilane on glass surface.

The methyltrimethoxysilane-treated glass surface was analyzed using XPS. The atomic concentrations determined from the XPS analysis did not show the presence of Na^+ ions which indicated that the glass surface was covered completely with the silane layer. Figure 8 shows the curve fitted C 1s spectrum of the silane-treated glass surface at 45° photoelectron take-off angle. The curve fit spectrum reveals that the major portion of the carbon is $Si—CH_3$ type carbon (75.74%) followed by a C—O type linkage (23.23%). The presence of this ether linkage indicates that there might have been unhydrolyzed methoxy groups ($Si—O—CH_3$) present in the silane layer. This type of methoxy group will not be present on the trimethylchlorosilane treated glass surfaces because the three methyl groups are not hydrolyzable. Thus, the adhesion data from the trimethylchlorosilane treated glass surfaces do not include any possible influence on adhesion by the presence of methoxy groups as might be the case in the methyltrimethoxysilane treated glass surfaces.

Blocks of several polyurethanes were cast on the silane-treated glass surface and were cured in the same manner as reported previously. These samples were tested for adhesion values and the data are shown in Table IX. A comparison of these data on glass surfaces completely blocked by the silane with adhesion data for the bare glass

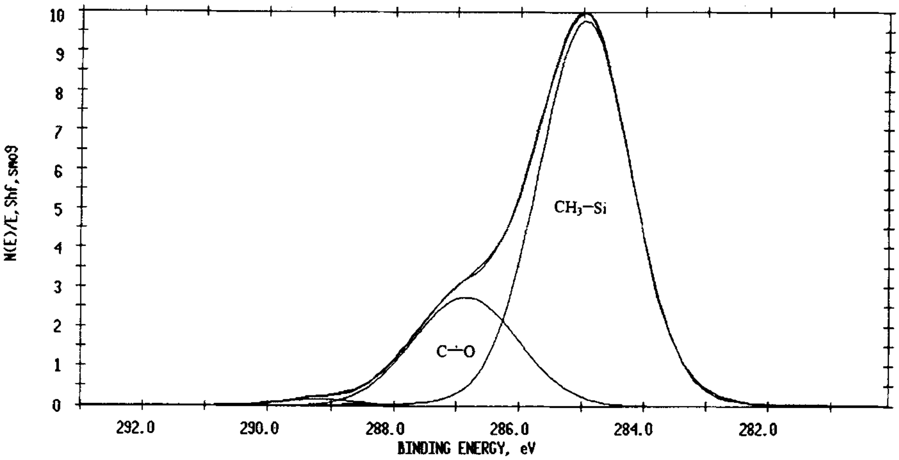

FIGURE 8 Curve fitted C 1s spectrum of methyltrimethoxysilane treated glass surface at 45° Photoelectron take-off angle.

TABLE IX
Adhesion values of various polyurethanes to silane treated glass surfaces

Samples	Adhesion to bare glass surface[9] (psi)/(MPa)	Adhesion to methyltrimethoxysilane treated glass surface (psi)/(MPa)	Adhesion to trimethyl chlorosilane treated glass surface (psi)/(MPa)
10D	4640 ± 80	4940 ± 390	4290 ± 310
	(32.5 ± 0.6)	(34.6 ± 2.7)	(30.0 ± 2.2)
5D	5240 ± 220	4790 ± 450	4740 ± 560
	(36.7 ± 1.5)	(33.5 ± 3.2)	(33.2 ± 3.9)
1D	2120 ± 530	2480 ± 440	2380 ± 550
	(5.78 ± 2.4)	(17.4 ± 3.1)	(16.7 ± 3.9)
10B	1590 ± 30	1470 ± 170	1370 ± 140
	(11.1 ± 0.2)	(10.3 ± 1.2)	(9.6 ± 1.0)

surface[9] reveals that the methyltrimethoxysilane coating on the glass surface had little influence on the adhesion values, within experimental error. Similar adhesion data are obtained from the trimethylchlorosilane treated glass surfaces. Both these data suggest that the adhesion mechanism of the polyurethanes to the glass surface is probably not due to covalent or ionic bonding in the interphase region.

The failed glass surface of the sample 10D from the methyltrimethoxysilane adhesion test was also analyzed using the XPS to determine the locus of failure. Table X shows the atomic concentrations of N, O, C and Si at three different photoelectron take-off-angles, 15°, 45°, and 90°. The presence of nitrogen reveals that nitrogen-containing species such as TDI and/or polyurethane linkages were present on the surface. Figure 9 shows the curve fitted C 1s spectra at 15°, 45°, and 90° photoelectron take-off angles. The peak at ~289.5 eV indicates that nitrogen is coming from the polyurethane linkages rather than from the TDI. The nitrogen concentration gradient increases with the sampling depth. This indicates that interdiffusion might have taken place between

TABLE X
O 1s, N 1s, C 1s, and Si 2p atomic percent concentrations at different photoelectron take-off angles for the adhesion failed 10D glass sample coated with methyltrimethoxysilane

Elements	Photoelectron take-off angle		
	15°	45°	90°
O	36.44	40.19	44.30
N	0.93	1.62	2.17
C	45.40	40.01	34.69
Si	17.23	18.19	18.84

the silane layer and the polyurethane matrix resulting in an interphase region. The locus of failure seems to be between the silane layer and the polyurethane matrix, through the interphase region. This interphase region observation is consistent with the previously made observations regarding interphase formation in the polyurethane/glass systems.[10]

Adhesion Mechanisms

Based on our previous studies regarding: the structure-property relationships in polyurethanes and their effects on adhesion; the phase separation in polyurethane and the formation of an interphase region between the polyurethanes and the glass surface,[9-10] and the observations made in this study regarding the role of physicochemical interactions in the interphase region, it can be inferred that the reversible physical interactions and not covalent chemical interactions in the interphase region play a key role in determining adhesion of the polyurethanes of this study to the soda-lime glass surfaces. The permanent dipole-dipole interactions and especially the hydrogen bonding between the polyurethane surface and glass surface appear to be very important for the overall adhesion. Phase separation in the matrix tends to cause a preferential segregation of BDO type species in the interphase region. Based on the linear relationship between the polar component (γ^P) of the surface free energy and the matrix adhesion, and the findings of the adhesion experiments with BDO -coated glass plaques, it can further be inferred that the presence of excess BDO in the interphase region influences matrix adhesion by increasing the modulus of the interphase region and by increasing the polar interactions with the glass surface.

To explore the roles of the increased interphase modulus and the increased polar interactions (hydrogen bonding) on adhesion, another experiment was conducted. In this experiment, the air sides of soda-lime glass plaques were coated with 2% (by weight) solution of trimethylchlorosilane in tetrahydrofuran solvent. After 30 minutes of air drying, some of the glass plaques were rinsed with tetrahydrofuran to remove any unbonded trimethylchlorosilane from the glass surfaces. The glass plaques thus prepared were overcoated with a 2% (by weight) solution of BDO in acetone and were allowed to dry at room temperature. The glass plaques were then evaluated for adhesion with 1D polyurethane and the data are shown in Table XI.

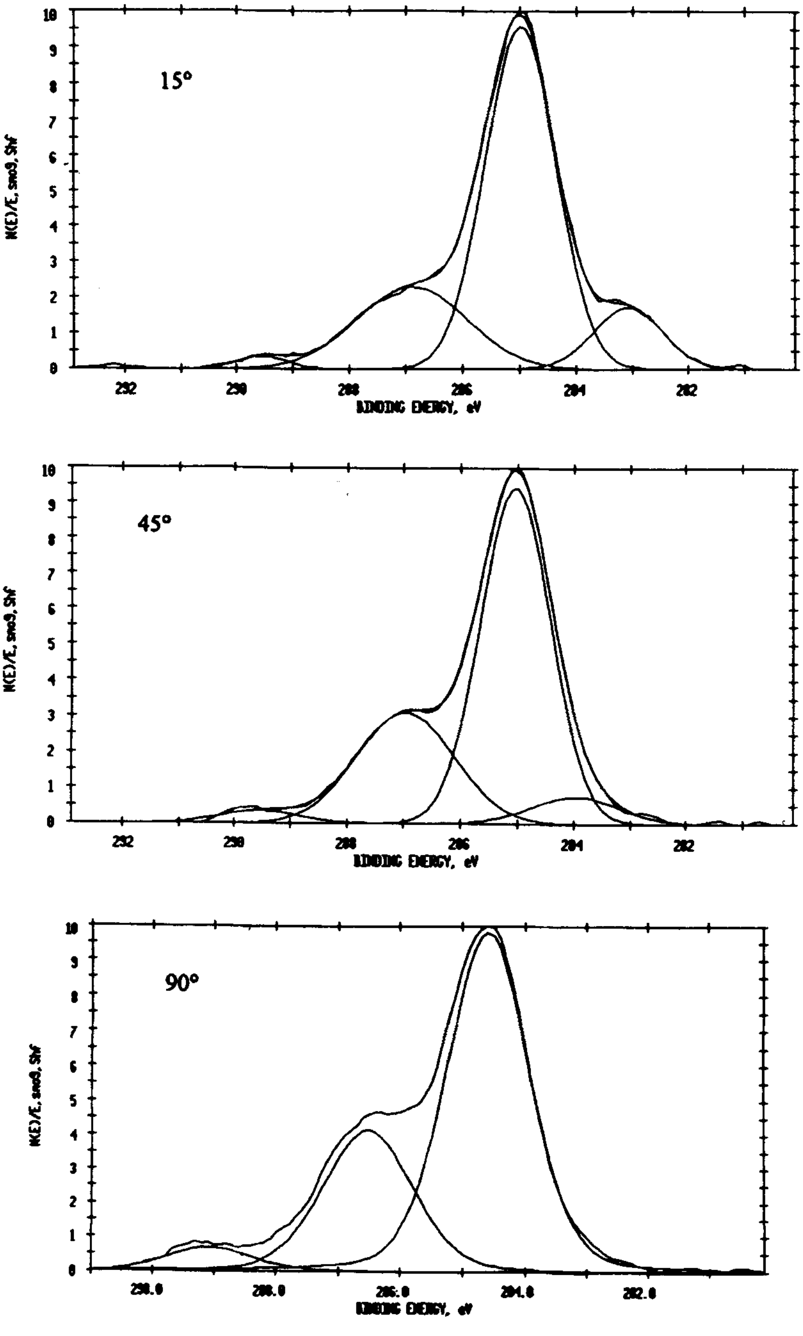

FIGURE 9 Curve fitted C 1s spectra of adhesion failed 10D glass samples precoated with methyltrimethoxysilane taken at 15°, 45°, and 90° photoelectron take-off angles.

TABLE XI
Adhesion values of 1D polyurethane to various treated glass surfaces

Glass treatments	Adhesion (psi)/(MPa)
Bare glass	2120 ± 530 (14.8 ± 3.7)
Glass coated with BDO	4980 ± 850 (34.9 ± 5.9)
Glass coated with trimethylchlorosilane	2380 ± 550 (16.7 ± 3.9)
Glass coated with trimethylchlorosilane and rinsed	2870 ± 530 (20.1 ± 3.7)
Glass coated with trimethylchlorosilane and overcoated with BDO	1570 ± 400 (11.0 ± 2.8)
Glass coated with trimethylchlorosilane and rinsed and overcoated with BDO	1780 ± 600 (12.5 ± 4.2)

The purpose of coating glass plaques with trimethylchlorosilane was to obtain an inert surface with which the possibility of hydrogen bonding with the subsequent coating of BDO can be minimized. In the case where the trimethylchlorosilane treated glass plaques were further rinsed with tetrahydrofuran, the possibilities of any potential polar interactions between the unbonded trimethylchlorosilane and the BDO were eliminated. In this fashion, the effect of increased interphase modulus due to excess BDO on the overall adhesion of the matrix can be studied. A comparison of the adhesion data between the BDO-coated glass plaques and the trimethylchlorosilane/BDO coated glass plaques reveals that the adhesion value went down from 4980 psi (34.3 MPa) to 1570 psi (10.8 MPa) when the BDO layer was devoid of potential hydrogen bonding with the glass surface. Similar results were obtained from the glass plaques treated with trimethylchlorosilane, rinsed and overcoated with BDO. This experiment suggests that hydrogen bonding between the excess butanediol hydroxyls in the interphase region and the glass surface is a necessary component of the mechanism of adhesion for phase-separated polyurethanes.

The suggested hydrogen bonding between BDO and the glass surface was further investigated using XPS. The air side of a soda-lime glass plaque was coated with a 2% (by weight) solution of BDO and was subjected to the polyurethane curing cycle (90°C for 24 hours). Afterwards, the glass plaque was rinsed several times with acetone to remove any unadsorbed BDO from the glass surface. A control sample was also subjected to the same procedure except for the BDO coating step. The curve fitted C1s spectra of the control sample and the BDO-coated sample are shown in Figure 10a and 10b, respectively. The bands at ~286.5 eV, associated with C-OH type species, indicate higher hydroxyl content (9.83%) on the BDO-treated sample as compared with the control sample (6.63%). This confirms that BDO can be adsorbed on the glass surfaces.

The hydrogen bonding in the interphase region can take place in numerous possible ways. One end of the butanediols can be hydrogen bonded to the carbamate linkages of the polyurethane groups and the other end can be hydrogen bonded with the glass surface hydroxyls. In another scenario, partially-reacted butanediols will have free

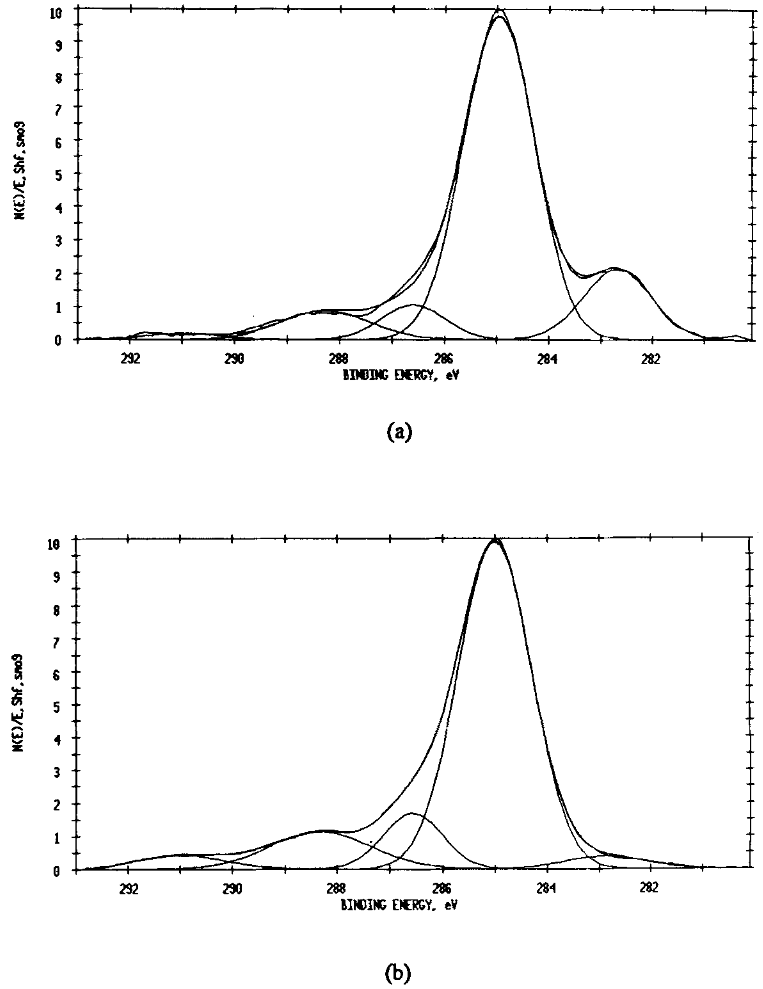

(a)

(b)

FIGURE 10 Curve fitted C 1s spectra of (a) control glass sample, (b) glass treated with BDO and rinsed.

hydroxyl groups to hydrogen bond with the glass surface. The polyester functionalities of the polyols and also the unreacted free hydroxyl ends of the polyols can potentially hydrogen bond with the glass surface. Yet another mechanism can be the direct hydrogen bonding of the polyurethane groups to the glass surface through the carbamate linkages of the polyurethane groups.

The preferential segregation of BDO at the interphase region observed in this study is not inconsistent with the previously reported studies. Hearn *et al.*[23] and Vargo *et al.*[1] have reported the enrichment of the air/polyurethane interface in low molecular weight polyether polyol components. The glass/polyurethane interphase of this study is expected to be different from the air/polyurethane interface studied by the above mentioned researchers. The high surface free energy (56.8 dynes/cm) and especially the polar nature of the glass surface ($\gamma^P = 37.6$ dynes/cm) will have a significant influence on the interphase composition. This reasoning is further supported by the studies reported by Deng and Schreiber[24] discussing orientation phenomena at polyurethane surfaces in contact with different media.

CONCLUSIONS

In this study, possible chemical and physical interactions at the polyurethane/glass interphase were explored. The contribution of chemical bonding, in the form of covalent and ionic bonding, on the overall glass/polyurethane adhesion was found to be not important. It was concluded that physical interactions are the most important factors in controlling glass/polyurethane adhesion. The polar component of surface free energy of the various polyurethanes correlated well with the XPS results regarding the BDO enrichment of the interphase regions in the phase-separated polyurethanes. The work of adhesion calculated from the surface free energy components of the polyurethanes and the glass surface was found to be a poor predictor of the actual adhesion behavior. However, a linear relationship between the polar surface free energy and the observed adhesion values emphasized the role of polar interactions on the adhesion.

The modulus of the interphase region was found to be higher than that of the matrix due to the preferential segregation of butanediol at the interphase. However, this increase in modulus alone was determined not to be the sole factor responsible for the increase in adhesion. It was concluded that the most important mechanism of adhesion between the polyurethanes and the glass surface of this study is through the formation of an interphase region in which hydrogen bonding between the butanediol-rich interphase region and the hydroxylated glass surface plays a key role.

Acknowledgements

The authors wish to thank the Donnelly Corporation, the office of Naval Research and the Automotive Composites Consortium for supporting this work. The authors also like to acknowledge the assistance of D. Hook in conducting the XPS experiments in this study.

References

1. T. G. Vargo, D. J. Hook, J. A. Gardella, Jr., M. A. Eberhardt, A. E. Meyer and R. E. Baier, *Appl. Spectroscopy* **45 (3)**, 448 (1991).
2. A. Sengupta and H. P. Schreiber, *J. Adhesion Sci. Technol.* **5 (11)**, 947 (1991).
3. F. M. Fowkes, D. W. Dwight and D. A. Cole, *J. Non-Crystalline Solids*, **120**, 47 (1990).
4. C. G. Pantano, *Ceramic Bull.*, **60(11)**, 1154 (1981).
5. D. J. Vaughan and R. C. Peek Jr., The Society of Plastics Industry, Inc., 29th Annual Tech. Conf., Sect. 13D, 1–4 (1974).
6. A. Lassas, L. E. Fagerholm, B. G. Stenlund and J. H. Nasman, *Polym. Compos.*, **14 (1)**, 1 (1993).
7. S. Markus and Z. Priel, *J. Coll. Interf. Sci.*, **82 (1)**, 150 (1981).
8. M. Mohai, I. Bertoti and M. Revesz, *Surf. Interf. Anal.*, **15**, 364 (1990).
9. R. K. Agrawal and L. T. Drazal, *J. Adhesion*, in press.
10. R. K. Agrawal and L. T. Drazal, *J. Adhesion Sci. Technol.*, in press (1994).
11. D. W. Van Krevelen, *Properties of Polymers*, 3rd Ed. (Elsevier Science Publishers, New York, 1990).
12. J. G. Eberhardt, *J. Phys. Chem.*, **70**, 1183 (1966).

13. J. Brandrup and E. H. Immergut, *Polymer Handbook* (John Wiley & Sons, New York, 1989).
14. S. Sugden, *J. Chem. Soc.*, **125**, 1177 (1924).
15. W. A. Zisman, *Contact Angle, Wettability and Adhesion*, Advances in Chemistry Symposium Series **43**, R.F. Gould, Ed. (ACS, Washington, DC, 1964).
16. J. Schultz, K. Tsutsumi and J. B. Donnet, *J. Coll. Interf. Sci.* **59**, 277 (1977).
17. F. M. Fowkes, in *Treatise on Adhesion and Adhesives*, Vol. 1, R. L. Patrick, Ed. (Marcel Dekker, New York, 1967), p. 352.
18. D. K. Owens and R. C. Wendt, *J. Appl. Polym. Sci.*, **13**, 1740 (1969).
19. D. H. Kaelble and K. C. Uy, *J. Adhesion*, **2**, 50 (1970).
20. D. H. Kaelble, *Physical Chemistry of Adhesion* (John Wiley & Sons, New York, 1971).
21. R. J. Good, in *Treatise on Adhesives*, Vol. 1, R. L. Patrick, Ed. (Marcel Dekker, New York, 1967), Chap. 2.
22. E. P. Plueddemann, *Silane Coupling Agents*, (Plenum Press, New York, 1991).
23. M. J. Hearn, B. D. Ratner and D. Briggs, *Macromolecules*, **21**, 2950–2959 (1988).
24. Z. Deng and H. P. Schreiber, *J. Adhesion*, **36**, 71–82 (1991).

APPENDIX A

Surface free energy estimation of the hard segment by the molar parachors

Groups	Number	P_S Sugden[11]	V_W(cm^2/mol) Van der Waals Volume[11]
$-CH_3$	1	56.1	13.67
Phenyl (trisubstituted)	1	155.8	40.80
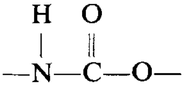 $-\overset{H}{\overset{\mid}{N}}-\overset{O}{\overset{\|}{C}}-O-$	2	94.4	18.0
$-CH_2-$	4	39.0	10.23
		$\Sigma P_S = 556.7$	$\Sigma V_W = 131.39$

$$\Sigma V = 1.6 \Sigma V_W = 210.22\,\text{cm}^3/\text{mol}$$

According to the molar parachor approach,

$$\gamma_H = \left(\frac{\Sigma P_S}{\Sigma V}\right)^4$$

$$\gamma_H = \left(\frac{556.7}{210.22}\right)^4 = 49.2\,\text{dynes/cm}$$